

Design and analysis of photonic optical switches with improved wavelength selectivity

Marcin Wielichowski^a, Sergiusz Patela^a

^aFaculty of Microsystems Electronics and Photonics, Wrocław University of Technology,
Poland

ABSTRACT

Efficient optical modulators and switches are the key elements of the future all-optical fiber networks. Aside from numerous advantages, the integrated optical devices suffer from excessive longitudinal dimensions. The dimensions may be significantly reduced with help of periodic structures, such as Bragg gratings, arrayed waveguides or multilayer structures. In this paper we describe methods of analysis and example of analytical results of a photonic switch with properties modified by the application of periodic change of effective refractive index. The switch is composed of a strip-waveguide directional coupler and a transversal Bragg grating.

Keywords: optical switch, all-optical devices, planar directional coupler, Bragg grating.

1. INTRODUCTION

Modern all optical network and future photonic systems will require miniaturized and efficient modulators, switches and other optical devices. Designs and devices known in principle for 20 years now, suffer from high longitudinal dimensions (from millimeters up to centimeters), which prohibits integration and cascading. One possible solution to this problem is application of periodic structures in the form of multilayers, Bragg gratings or arrayed waveguides. At its extreme, one may consider making use of 3D photonic crystals – however due to extreme (sub-nanometer) design tolerances – this is not the approach of choice for most of the popular applications. Application of periodic structure may decrease dimensions of the devices, improve working efficiency and wavelength selectivity. It is interesting to notice, that the periodicity may be applied in all of the three dimensions independently, each periodicity affecting propagation in different way. However, design and analysis of structures with a few independent periodicities poses significant challenges, calling for new methods of analysis or at least adaptation of a known ones. In this paper we describe semi-analytical method that is capable to analyze light propagation in arbitrary integrated optic structure, composed of multilayer waveguides, gratings and coupled waveguides. Refractive index changes induced by the control optical beam are taken into account also, so that our method is capable of analysis of all optical devices.

Analysis is performed with the transfer matrix method and effective index methods. Combination of both methods is used to calculate transversal optical field distribution and longitudinal propagation constants of eigenmodes guided by the structure. Then the transfer-matrix method is applied to calculate the propagation of the guiding structure eigenmodes alongside the longitudinal direction. The transfer-matrix technique for the analysis of a contra-directional grating-assisted coupler is based on [1]. Details concerning the reflection coefficients come from [2] and [3]. A method, also based on the transfer-matrix technique, of calculating the 1D distributions of electromagnetic fields is described in detail in [4] and [5].

The results obtained by us include transmission and reflection characteristics of the switches, with dependencies on the signal-beam wavelength and refractive index change induced by the control-beam optical power. The assumed physical properties of the structure correspond to a semiconductor heterostructure of GaInNAs / GaAs composition with superlattice active layer. Results of analysis and measurements of an all-optical switch based on the directional coupler loaded with Bragg grating, manufactured in GaInAs / InP can be found in [6].

2. STRUCTURE

Two vertical cross-sections of a planar structure being analyzed are shown in Fig. 1. First, two arms of the directional coupler are formed as strip waveguides by etching to a depth of d_{strip} . Then, by etching to a depth of d_{Bragg} , Bragg grating is formed on top of both strip waveguides and on surfaces surrounding them. Grating teeth will be marked throughout the rest of the article as + sections, and spaces between teeth as – sections.

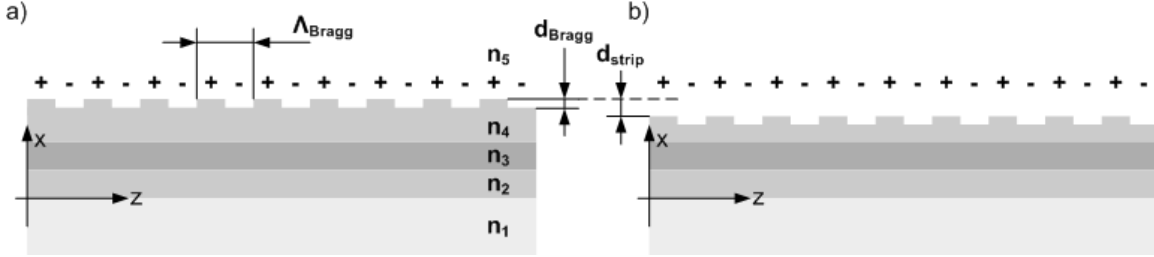


Fig. 1. Contra-directional grating-assisted coupler - vertical cross-section of a) one of coupler arms (a strip waveguide) and b) area surrounding coupler arms..

For the purpose of simplicity, the superlattice active layer has been reduced to a single layer with the refractive index n_3 . Presentation of methods of such replacement is given e.g. in [7] and [8].

3. METHOD OF ANALYSIS

A top view of structure from Fig. 1. is shown in Fig. 2. Method of analysis applied by the authors follows in the next chapter.

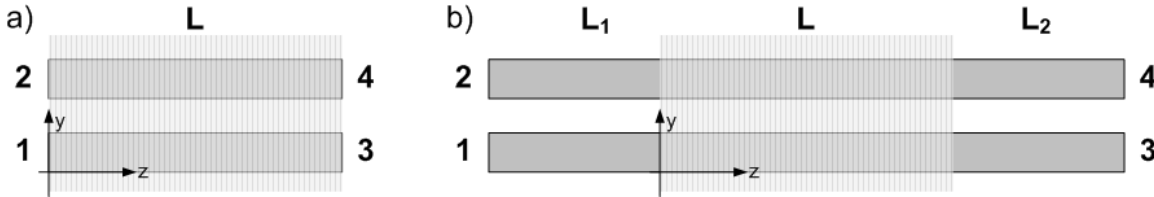


Fig. 2. Schematic view of a) contra-directional grating-assisted coupler and b) contra-directional grating-assisted coupler accompanied by input and output directional couplers.

Let us define column vectors of (complex) field amplitudes at section interfaces z_k . Amplitudes in section + are:

$A_+ = [A_+^{fs}, A_+^{fa}, A_+^{bs}, A_+^{ba}]^{TR}$ and in section - : $A_- = [A_-^{fs}, A_-^{fa}, A_-^{bs}, A_-^{ba}]^{TR}$. Indexes s, a and f, b denote: symmetric or asymmetric modes propagating forward or backward, respectively. For each section interface we define transmission matrices transforming the field amplitudes from the left side of the interface to the right side of the interface. Depending on section sequence at given z_k , + / - or - / +, two types of matrices are possible: T_{+-} and T_{-+} . They act as follows:

$$A_- = T_{+-} A_+ \quad (3.1a)$$

$$A_+ = T_{-+} A_- \quad (3.1b)$$

Explicitly, the transmission matrices are given as:

$$T_{+-} = \begin{bmatrix} t_+^{ss} & t_+^{sa} & t_-^{ss} & t_-^{sa} \\ t_+^{as} & t_+^{aa} & t_-^{as} & t_-^{aa} \\ t_-^{ss} & t_-^{sa} & t_+^{ss} & t_+^{sa} \\ t_-^{as} & t_-^{aa} & t_+^{as} & t_+^{aa} \end{bmatrix}, T_{-+} = \begin{bmatrix} t_+^{ss} & t_+^{sa} & -t_-^{ss} & -t_-^{sa} \\ t_+^{as} & t_+^{aa} & -t_-^{as} & -t_-^{aa} \\ -t_-^{ss} & -t_-^{sa} & t_+^{ss} & t_+^{sa} \\ -t_-^{as} & -t_-^{aa} & t_+^{as} & t_+^{aa} \end{bmatrix} \quad (3.2)$$

where elements of the type ss and aa are amplitude transmission or reflection coefficients for symmetric or antisymmetric modes, respectively. Coefficients of the type sa and as are amplitude coefficients of coupling from symmetric to antisymmetric and from antisymmetric to symmetric modes, respectively, due to mode unorthogonality at section interfaces. In numerical results given in section 4. we assume modes to be orthogonal, thus the sa and as coefficients are set to 0. With mode orthogonality assumed, the coefficients ss and aa can be derived directly from Fresnel reflection coefficients. It is enough to calculate them only for the $+/-$ interface (and then substitute to T_{-+} with sign change at each t_-):

$$t_+ = (N_L + N_R)/(2 * N_R) \quad (3.3a)$$

$$t_- = (N_L - N_R)/(2 * N_R) \quad (3.3b)$$

N_L and N_R are effective refractive coefficients (or equally propagation constants) in section to the left and to the right of section interface, respectively. E.g. $t_+^{ss} = (\gamma_+^s + \gamma_-^s)/(2 * \gamma_+^s)$.

For all sections $+$ and $-$ we then define transfer matrices describing phase change of light wave due to propagation over a distance equal to the length of given section. The transfer matrices are:

$$P_+ = \text{diag}[\exp(-i\gamma_+^s \Lambda_+) \quad \exp(-i\gamma_+^a \Lambda_+) \quad \exp(i\gamma_+^s \Lambda_+) \quad \exp(i\gamma_+^a \Lambda_+)] \quad (3.4a)$$

$$P_- = \text{diag}[\exp(-i\gamma_-^s \Lambda_-) \quad \exp(-i\gamma_-^a \Lambda_-) \quad \exp(i\gamma_-^s \Lambda_-) \quad \exp(i\gamma_-^a \Lambda_-)] \quad (3.4b)$$

Now we write down a matrix relating field amplitudes at the beginning and at the end of grating's period:

$$T_{++} = T_{-+} P T_{+-} P_+ \quad (3.5)$$

For entire grating-assisted coupler, a matrix relating field amplitudes at both sides of the device, is a product of all matrices T_{++} :

$$T_{++}^N = T_{++}(z_1) T_{++}(z_3) T_{++}(z_5) \dots \quad (3.6)$$

Summarizing, the matrix T_{++}^N acts as follows:

$$A_+(0) = T_{++}^N A_+(L) \quad (3.7)$$

To describe the phase change of light wave during propagation through input and output couplers we will now define two transfer matrices T_1 and T_2 , which are similar to P_+ and P_+ written earlier for individual grating sections:

$$T_1 = \text{diag}[\exp(-i\gamma_1^s L_1) \quad \exp(-i\gamma_1^a L_1) \quad \exp(i\gamma_1^s L_1) \quad \exp(i\gamma_1^a L_1)] \quad (3.8a)$$

$$T_2 = \text{diag}[\exp(-i\gamma_2^s L_2) \quad \exp(-i\gamma_2^a L_2) \quad \exp(i\gamma_2^s L_2) \quad \exp(i\gamma_2^a L_2)] \quad (3.9b)$$

Transfer matrix T for entire device, i.e. the grating assisted coupler and the in and out couplers, is:

$$T = T_2 T_{++}^N T_1 \quad (3.10)$$

The transfer matrix T relates field amplitudes at one side of the device to field amplitudes at the other side. However, to be able to calculate output powers from given input powers, a scattering matrix instead of the transfer matrix is needed. Formulas relating the scattering matrix S to the transfer matrix T are:

$$T = \begin{bmatrix} T_{11} & T_{12} \\ T_{21} & T_{22} \end{bmatrix}, S = \begin{bmatrix} S_{11} & S_{12} \\ S_{21} & S_{22} \end{bmatrix} \quad (3.11)$$

where:

$$S_{11} = T_{11} - T_{12}T_{22}^{-1}T_{21}, \quad S_{12} = T_{12}T_{22}^{-1}, \quad S_{21} = T_{22}^{-1}T_{21}, \quad S_{22} = T_{22}^{-1} \quad (3.12)$$

Writing a column vectors of input field amplitudes

$A_{IN} = [A_1^{fs}(-L_1), A_1^{fa}(-L_1), A_2^{bs}(L+L_2), A_2^{ba}(L+L_2)]^{TR}$ and of output field amplitudes:

$A_{OUT} = [A_1^{fs}(L+L_2), A_1^{fa}(L+L_2), A_2^{bs}(-L_1), A_2^{ba}(-L_1)]^{TR}$ the effect of the scattering matrix S can be expressed as follows:

$$A_{OUT} = SA_{IN} \quad (3.13)$$

All the above derivations concerned coupler eigenmodes. To calculate optical powers exiting the device through individual ports 1,...,4 we need to carefully define a method of calculating the optical power exiting a port. We will assume the following definition:

$$P_n = \int_{y_{left}}^{y_{right}} |A^s \Phi^s(y) + A^a \Phi^a(y)|^2 dy \quad (3.14)$$

where A^s, A^a are field amplitudes and $\Phi^s(y), \Phi^a(y)$ are field distributions of symmetric and antisymmetric coupler-eigenmodes exiting the given port n . Coordinates of walls of port's strip waveguide are y_{left}, y_{right} .

Using the above definition we can calculate waveguide-to-coupler and coupler-to-waveguide coupling matrices. The waveguide-to-coupler C_{WC} and coupler-to-waveguide C_{CW} amplitude coupling matrices have the following form:

$$C_{WC} = \begin{bmatrix} C_{WC-1} & [0] \\ [0] & C_{WC-2} \end{bmatrix}, C_{CW} = \begin{bmatrix} [0] & C_{CW-1} \\ C_{CW-2} & [0] \end{bmatrix} \quad (3.15)$$

where:

$$C_{WC-1} = \begin{bmatrix} \Phi_{W1} \rightarrow \Phi_1^s & \Phi_{W2} \rightarrow \Phi_1^s \\ \Phi_{W1} \rightarrow \Phi_1^a & \Phi_{W2} \rightarrow \Phi_1^a \end{bmatrix}, C_{WC-2} = \begin{bmatrix} \Phi_{W3} \rightarrow \Phi_2^s & \Phi_{W4} \rightarrow \Phi_2^s \\ \Phi_{W3} \rightarrow \Phi_2^a & \Phi_{W4} \rightarrow \Phi_2^a \end{bmatrix} \quad (3.16)$$

$$C_{CW-1} = \begin{bmatrix} \Phi_1^s \rightarrow \Phi_{W1} & \Phi_1^a \rightarrow \Phi_{W1} \\ \Phi_1^s \rightarrow \Phi_{W2} & \Phi_1^a \rightarrow \Phi_{W2} \end{bmatrix}, C_{CW-2} = \begin{bmatrix} \Phi_2^s \rightarrow \Phi_{W3} & \Phi_2^a \rightarrow \Phi_{W3} \\ \Phi_2^s \rightarrow \Phi_{W4} & \Phi_2^a \rightarrow \Phi_{W4} \end{bmatrix} \quad (3.17)$$

Here we have used the symbol \rightarrow to denote coupling between field distributions. Values of individual couplings are given by overlap integrals with integration limits y_{left}, y_{right} being the coordinates of walls of port's strip waveguide:

$$\Phi_{Wm} \rightarrow \Phi_n^t = \int_{y_{left}}^{y_{right}} \Phi_{Wm}(y) \Phi_n^t(y)^* dy, \quad \Phi_n^t \rightarrow \Phi_{Wm} = \int_{y_{left}}^{y_{right}} \Phi_n^t(y) \Phi_{Wm}(y)^* dy \quad (3.18)$$

where: $m \in \{1,2,3,4\}$, $n \in \{1,2\}$ and $t \in \{s, a\}$. All the field distributions are normalized:

$$\int_{-\infty}^{+\infty} \Phi_n^t(y) \Phi_n^t(y)^* dy = 1, \quad \int_{-\infty}^{+\infty} \Phi_{Wm}(y) \Phi_{Wm}(y)^* dy = 1 \quad (3.19)$$

Finally, using matrices defined until now we can express waveguide eigenmode amplitudes exiting the coupler by waveguide eigenmode amplitudes entering the coupler. Appropriate formula is:

$$A_{W-OUT} = C_{CW} S C_{WC} A_{W-IN} \quad (3.20)$$

4. NUMERICAL RESULTS

As an example, we will give numerical results for three different configurations of the discussed structure, having different, potentially useful, characteristics. All three configurations are summarized in Table 1. Schematic view of signal beam flow within the device in different configurations is shown in Figure 3.

No.	Input coupler	Grating-assisted coupler / length [μm]	Bragg grating / length [μm]	Output coupler	Active port(s) – no stimulation	Active port(s) – with stimulation
1.	no	$0.5 * \text{beat length} / 1200$	full reflection, apodized / 1200	no	2	4
2.	$0.5 * \text{beat length}$	$0.5 * \text{beat length} / 1200$	full reflection, apodized / 1200	no	2	3
3.	no	$0.5 * \text{beat length} / 1200$	full reflection, apodized / 1200	$0.25 * \text{beat length}$	2	3 and 4 (power splitter)

Tab. 1. Summary of device configurations analyzed.

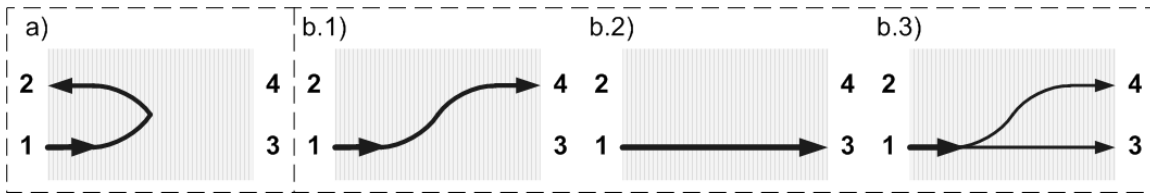


Fig. 3. Schematic view of signal beam flow in different configurations a) without control-beam stimulation b) with control-beam stimulation in configurations 1., 2. and 3., respectively.

The calculations were conducted for a system of layers shown in Figure 1. Refraction coefficients values $n_1 = 3.4$, $n_2 = n_4 = 3.35$, $n_3 = 3.55$ and $n_5 = 1.0$, layer thicknesses $t_2 = 2.0\mu\text{m}$, $t_3 = 0.4\mu\text{m}$, $t_4 = 0.3\mu\text{m}$, etching depths $d_{strip} = 0.11\mu\text{m}$, $d_{Bragg} = 0.09\mu\text{m}$, widths of both strip waveguides $2.00\mu\text{m}$ and separation between waveguides $2.58\mu\text{m}$. The value of separation has been adjusted so that half the beat length of the grating-assisted coupler equals $1200\mu\text{m}$. The Bragg grating without apodization requires a length of only $400\mu\text{m}$ to achieve full reflection. However, since the apodization decreases the reflectivity of the grating, we have assumed the apodized-grating length to be three times bigger, i.e. $1200\mu\text{m}$, than the length required for a grating without apodization. Grating period is $0.189\mu\text{m}$. Apodization has been achieved through modulation of the grating duty cycle. The modulation formula is $0.5 + 0.4\text{Cos}(\pi/N * z)$ where N is the number of grating's periods. Reflection and transmission curves of power carried by eigenmodes of grating-assisted coupler described above, are shown in Fig. 4.

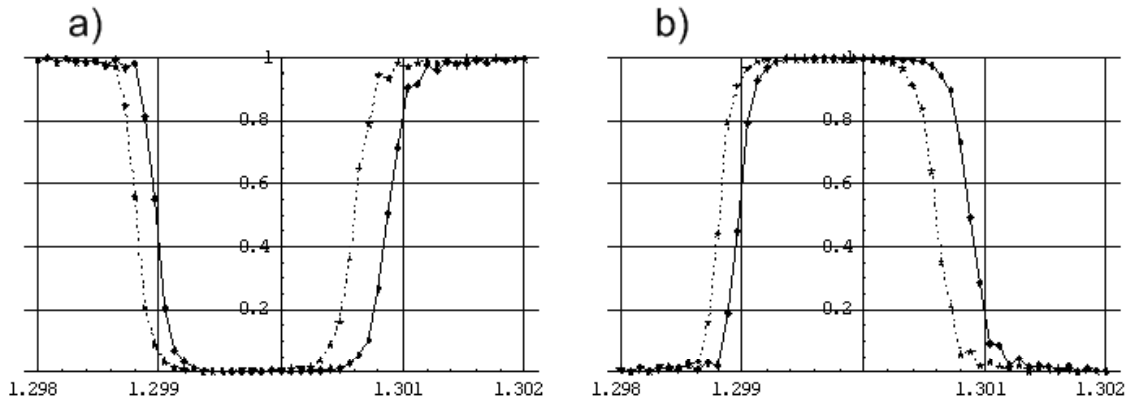


Fig. 4. Power reflection and transmission curves of two eigenmodes guided by the analyzed grating-assisted coupler: symmetric eigenmode (solid line) and antisymmetric eigenmode (dotted line).

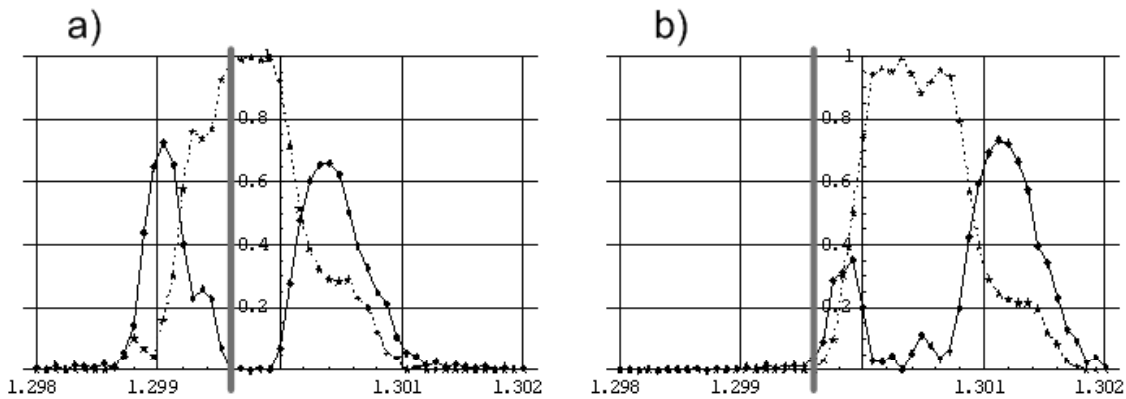


Fig. 5. Optical power exiting the device through port 1. (solid line) and port 2. (dotted line) a) without stimulation and b) under stimulation with the control beam.

According to the analysis discussed in section 3., optical powers exiting individual ports of the device have been calculated. Fig. 5. contains results for the device configuration 1. There is shown power exiting through port 1., i.e. power reflected to the signal-beam source, and power exiting through port 2. To demonstrate the impact of refractive index modulation on individual ports of the device, Fig. 5. shows both the device's response without stimulation (Fig. 5.a) and under stimulation with the control beam (Fig. 5.b). Calculations for the stimulated state assume a change of the refractive index of the active layer (n_3) in both arms of the coupler by a value of $4.0 \cdot 10^{-3}$. The thick vertical line in both plots marks a wavelength chosen to be the signal-beam wavelength. By comparing Fig. 5.a and 5.b it is clearly visible that the discussed control-beam stimulation shifts the device's response towards longer light wavelength. In current example the shift is about $1.0nm$. Thus, using the control beam it is possible to change the distribution of the signal-beam optical power among ports of the device. In this example, when the control beam is on, optical power ceases exiting through port 2. (and starts exiting through port 4. – also see Tab. 1 and Fig. 3.). The shape of the shifted response undergoes a change, but it does not affect the functioning of the device.

Plots of the optical power exiting through ports 3. and 4. in the device configurations 1., 2. and 3. are shown in Fig. 6.

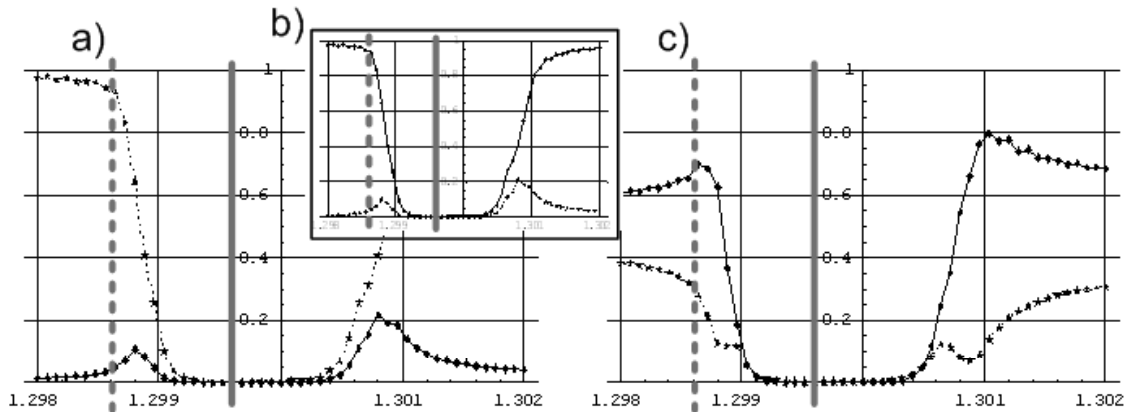


Fig. 6. Optical power exiting the device through port 3. (solid line) and port 4. (dotted line) without stimulation (solid vertical line) and under stimulation (dashed vertical line) with the control beam in device configurations a) 1., b) 2. and c) 3

It must be noted that the relatively large refractive index change required for functioning of the presented device might be decreased by optimizing the geometrical parameters of the device (e.g. to increase the power confinement factor in the active layer's volume stimulated by the control beam).

5. CONCLUSIONS

We have described in details a method of calculating the scattering matrix for the eigenmodes of a contra-directional grating-assisted coupler. Also calculation of the waveguide-to-coupler and coupler-to-waveguide coupling of eigenmodes has been discussed. Based on the presented methods, a structure of the contra-directional grating-assisted coupler with exemplary physical parameters, has been analyzed. The structure has been shown to potentially function as an all-optical switch allowing various possible output-port characteristics depending on additional elements – directional couplers – used in the construction of the device. In future, the method will be applied to design and optimize structure and technology of semiconductor photonic devices.

REFERENCES

1. J. Hong, W. Huang, *Contra-directional coupling in grating-assisted guided-wave devices*, Journal of Lightwave Technology, vol. 10, no. 7, pp. 873-881, 1992
2. T. Makino, *Effective-index matrix analysis of distributed feedback semiconductor lasers*, IEEE Journal of Quantum Electronics, vol. 28, no. 2, pp. 434-440, 1992
3. T. Makino, *Threshold condition of DFB semiconductor lasers by the local-normal-mode transfer-matrix method: correspondence to the coupled-wave method*, Journal of Lightwave Technology, vol. 12, no. 12, pp. 2092-2099, 1994
4. K.-H. Schlereth, M. Tacke, *The complex propagation constant of multilayer waveguides: an algorithm for a personal computer*, IEEE Journal of Quantum Electronics, vol. 26, no. 4, pp. 627-630, 1990
5. T.D. Visser, H. Blok, D. Lenstra, *Modal analysis of a planar waveguide with gain and losses*, IEEE Journal of Quantum Electronics, vol. 31, no. 10, pp. 1803-1810, 1995
6. C. Coriasso, D. Campi, L. Faustini, A. Stano, C. Cacciatore, *Optically controlled contradirectional coupler*, IEEE Journal of Quantum Electronics, vol. 35, no. 3, pp. 298-305, 1999
7. G.M. Alman, L.A. Molter, H. Shen, M. Dutta, *Refractive index approximations from linear perturbation theory for planar MQW waveguides*, IEEE Journal of Quantum Electronics, vol. 28, no. 3, pp. 650-657, 1992
8. R.E. Smith, L.A. Molter, M. Dutta, *Evaluation of refractive index approximations used for mode determination in multiple quantum well slab waveguides*, IEEE Journal of Quantum Electronics, vol. 27, no. 5, pp. 1119-1122, 1991